



Different Cortical Gyrfication Patterns in Alzheimer's Disease and Impact on Memory Performance

Christian Núñez, PhD ^{1,2}, Antonio Callén, MD,^{1,2} Federica Lombardini, MSc,^{1,2}
Yaroslau Compta, PhD, MD,^{3,4,5} and Christian Stephan-Otto, PhD, ^{1,2,6}
for the Alzheimer's Disease Neuroimaging Initiative[†]

Objective: The study of cortical gyrfication in Alzheimer's disease (AD) could help to further understanding of the changes undergone in the brain during neurodegeneration. Here, we aimed to study brain gyrfication differences between healthy controls (HC), mild cognitive impairment (MCI) patients, and AD patients, and explore how cerebral gyrfication patterns were associated with memory and other cognitive functions.

Methods: We applied surface-based morphometry techniques in 2 large, independent cross-sectional samples, obtained from the Alzheimer's Disease Neuroimaging Initiative project. Both samples, encompassing a total of 1,270 participants, were analyzed independently.

Results: Unexpectedly, we found that AD patients presented a more gyrficated entorhinal cortex than HC. Conversely, the insular cortex of AD patients was hypogyrficated. A decrease in the gyrfication of the insular cortex was also found in older HC participants as compared with younger HC, which argues against the specificity of this finding in AD. However, an increased degree of folding of the insular cortex was specifically associated with better memory function and semantic fluency, only in AD patients. Overall, MCI patients presented an intermediate gyrfication pattern. All these findings were consistently observed in the two samples.

Interpretation: The marked atrophy of the medial temporal lobe observed in AD patients may explain the increased folding of the entorhinal cortex. We additionally speculate regarding alternative mechanisms that may also alter its folding. The association between increased gyrfication of the insular cortex and memory function, specifically observed in AD, could be suggestive of compensatory mechanisms to overcome the loss of memory function.

ANN NEUROL 2020;00:1–14

Whereas brain volume deficits have been largely explored in Alzheimer's disease (AD),¹ the examination of other brain features such as cortical folds, that is, brain gyrfication, has generated less interest. The analysis of cortical folds could provide interesting information on

the underlying cytoarchitecture^{2,3} and connectivity of the brain,⁴ which are probably altered in neurodegenerative diseases as a consequence of widespread brain atrophy. These alterations are likely to leave footprints in brain shape that are not captured with more traditional

View this article online at wileyonlinelibrary.com. DOI: 10.1002/ana.25741

Received Nov 11, 2019, and in revised form Apr 3, 2020. Accepted for publication Apr 4, 2020.

Address correspondence to Dr Stephan-Otto, C/Doctor Antoni Pujadas, 42, 08830 Sant Boi de Llobregat, Barcelona, Spain.

E-mail: cstephanotto@pssjd.org

[†]Data used in preparation of this article were obtained from the Alzheimer's Disease Neuroimaging Initiative (ADNI) database (adni.loni.usc.edu). As such, the investigators within the ADNI contributed to the design and implementation of ADNI and/or provided data but did not participate in the analysis or writing of this report. A complete listing of ADNI investigators can be found at: http://adni.loni.usc.edu/wp-content/uploads/how_to_apply/ADNI_Acknowledgement_List.pdf

From the ¹Parc Sanitari Sant Joan de Déu, Sant Boi de Llobregat, Barcelona, Spain; ²Institut de Recerca Sant Joan de Déu, Esplugues de Llobregat, Barcelona, Spain; ³Parkinson's Disease & Movement Disorders Unit, Neurology Service, Hospital Clínic de Barcelona & Maria de Maeztu Excellence Center Institute of Neuroscience, University of Barcelona, Barcelona, Spain; ⁴Institute of Biomedical Research August Pi i Sunyer (IDIBAPS), Barcelona, Spain; ⁵Centro de Investigación Biomédica en Red sobre Enfermedades Neurodegenerativas (CIBERNED: CB06/05/0018-ISCI), Barcelona, Spain; and ⁶Centro de Investigación Biomédica en Red de Salud Mental (CIBERSAM), Madrid, Spain

Additional supporting information can be found in the online version of this article.

volumetric analyses but that could be detected with cortical gyrification analyses.

Increased cortical folding in several brain regions has been associated with better intelligence scores.^{5–7} Similarly, from an evolutionary perspective, it seems clear that those animal species typically considered more intelligent (eg, primates and cetaceans) show more gyrified brains.^{8,9} Although the cerebral cortex folds during the prenatal stage, changes in the cortical surface occur throughout life.⁴ The study of brain gyrification in dementia may therefore contribute to improved understanding of the changes that the brain undergoes during the neurodegenerative process, and what clinical and functional consequences they may have.

The scarcely available literature on brain gyrification and AD^{10–18} presents several limitations. First, most studies either have employed highly nonspecific measures, such as global gyrification indices accounting for complete cerebral lobes, or have examined only specific, predefined sulci, which introduces a potential bias and limits the ability to develop a wider picture of the cortical gyrification differences between controls and patients. Only a few studies have utilized a whole-cortex approach,^{14,17,18} although they employed rather small samples. Second, there are no studies at all addressing the relation between cortical gyrification and memory in a specific sample of mild cognitive impairment (MCI) or AD patients. Finally, several potential confounding factors, such as education level and medication, have generally not been controlled for.

Here, we present a report in which we generated whole-cortex gyrification index (GI) maps aiming to thoroughly analyze gyrification differences between healthy controls (HC) and patients with MCI or AD. We also aimed to explore whether the degree of cortical gyrification of specific cerebral regions was associated with memory function in patients. To this end, we employed 2 large, independent samples coming from the Alzheimer's Disease Neuroimaging Initiative (ADNI) project, attempting to produce reliable and robust results. We expected to find regions of decreased gyrification in AD patients compared with HC, mainly confined to temporal cortical regions. We also hypothesized that MCI patients would show an intermediate cortical gyrification pattern between HC and AD. Given the lack of literature, the analysis of gyrification and memory function was mainly exploratory.

Subjects and Methods

Participants

We included a total of 1,270 participants in the study coming from the ADNI. Of these, 785 participants were selected from

the ADNI-1 project (223 HC, 384 MCI, 178 AD), and 485 from the ADNI-2 project (183 HC, 159 MCI, 143 AD). All participants belonged to only one of the two projects. The ADNI (<http://adni.loni.usc.edu>) was launched in 2003 as a public–private partnership, led by principal investigator Michael W. Weiner, MD. All the inclusion and exclusion criteria of the ADNI-1 and ADNI-2 projects, as well as the criteria employed for the classification of the participants in the different groups, can be found at the ADNI website (<http://adni.loni.usc.edu/methods/documents>). The ADNI study was conducted according to Good Clinical Practice guidelines, the Declaration of Helsinki, and US 21CFR Part 50–Protection of Human Subjects and Part 56–Institutional Review Boards, and pursuant to state and federal HIPAA regulations. Written informed consent for the study was obtained from all subjects and/or authorized representatives and study partners before protocol-specific procedures were carried out.

Neuroimaging Data Acquisition and Processing

We obtained the high-resolution 3-dimensional T₁-weighted structural images acquired at the first (baseline) visit of the participants. All the structural images included from ADNI-1 were acquired with 1.5T scanners, whereas those included from ADNI-2 were acquired with 3T scanners. The detailed magnetic resonance imaging (MRI) protocols of the ADNI project can be consulted at the ADNI website (<http://adni.loni.usc.edu/methods/documents> and <http://adni.loni.usc.edu/methods/documents/mri-protocols>). We processed all the structural images entirely with the CAT toolbox (<http://www.neuro.uni-jena.de/cat>), implemented in SPM12 (<http://www.fil.ion.ucl.ac.uk/spm>), which runs under MATLAB (release 2012b; MathWorks, Natick, MA). Image processing included gray matter (GM), white matter (WM), and cerebrospinal fluid (CSF) segmentation, and the reconstruction of the cortical surface for each participant. GM volumes for specific brain structures were automatically calculated using the Neuromorphometrics atlas (<http://www.neuromorphometrics.com>). Cortical reconstruction resulted in the creation of a mesh of the central cortical surface, which is the surface located between the inner (WM/GM boundary) and the outer (GM/CSF boundary) cortical surfaces. The central surface provides a good representation of the cortex and allows one to accurately estimate cortical parameters.¹⁹ GI maps were then estimated according to the procedure described by Luders et al,²⁰ which relies on the mean curvature values from each vertex of the surface mesh. We resampled the GI maps to a high-resolution 164k mesh, and we smoothed them by applying a 22mm full width at half maximum (FWHM) filter. We used these resampled and smoothed GI maps for the whole-cortex surface-based morphometry (SBM) analyses of gyrification described later in the Statistical Analysis section. These whole-cortex SBM analyses of the GI maps allowed us to identify gyrification differences throughout the brain on a vertexwise basis. We chose the Desikan-Killiany (DK40)²¹ as the reference atlas. GM volume and cortical thickness maps (smoothed with 8mm and 15mm FWHM filters, respectively, following CAT software recommendations) were also computed for

complementary analyses. The CAT toolbox is regarded as a reliable alternative to other more established surface-analysis software, such as FreeSurfer,²² and has been employed for gyrfication analysis in several recent publications (eg, Besteher et al²³ and Spalhoff et al²⁴).

Data Processing Quality Control

We carried out a 2-step quality control procedure aiming to identify and potentially exclude participants whose processed imaging data raised serious concerns. In the first step, we utilized the Check Sample Homogeneity tool for voxel-based morphometry (VBM) data from the CAT toolbox, separately for the ADNI-1 and ADNI-2 samples, to detect participants having abnormal GM segmentations as compared with the rest of the sample. In the second step, we applied the Check Sample Homogeneity tool

for surface data on the resampled and smoothed GI maps to detect possible surface reconstruction defects. Following each step, we visually inspected those GM segmentations and/or GI maps identified as potentially defective. We excluded from the study those participants with confirmed abnormal GM segmentations and/or GI maps. Of the initial sample of 1,320 participants, we excluded 27 participants after the first quality control step (15 from ADNI-1 and 12 from ADNI-2), and 23 after the second step (18 from ADNI-1 and 5 from ADNI-2), which resulted in the final sample of 1,270 participants.

Neuropsychological Tests and Cognitive Outcomes

To assess memory and other cognitive capacities, we obtained performance scores from 5 neuropsychological tests, for which

TABLE 1. Sociodemographic, Clinical, and Cognitive Data Comparison between HC, MCI, and AD Patients from the ADNI-1 Sample

	ADNI-1, n = 785			Differences
	HC, n = 223	MCI, n = 384	AD, n = 178	
Age, yr	75.99 ± 5.05	74.81 ± 7.45	75.17 ± 7.55	None ^a
Age range	60–90	55–89	55–91	—
Sex, M/F	115/108	244/140	91/87	MCI ≠ (HC/AD) ^{b,c}
Education, yr	16.02 ± 2.86	15.60 ± 3.05	14.58 ± 3.15	(HC/MCI) > AD ^{a,d}
Ethnicity, white/other	204/19	361/23	167/11	None ^b
Handedness, right-/left-handed	207/16	351/33	167/11	None ^b
Cumulative medication until scan, mg/yr ^e	—	9.56 ± 18.57	27.87 ± 32.20	AD > MCI ^{a,d}
RAVLT sum trials 1–5	43.43 ± 9.11	30.41 ± 8.82	23.50 ± 7.54	HC > MCI > AD ^{d,f}
RAVLT delayed score	7.50 ± 3.74	2.77 ± 3.20	0.74 ± 1.67	HC > MCI > AD ^{d,f}
Mini-Mental State Examination score	29.12 ± 0.98	27.00 ± 1.77	23.29 ± 2.01	HC > MCI > AD ^{d,f}
Immediate Logical Memory score	13.80 ± 3.53	7.06 ± 3.14	4.22 ± 2.90	HC > MCI > AD ^{d,f}
Delayed Logical Memory score	12.94 ± 3.64	3.75 ± 2.62	1.30 ± 1.88	HC > MCI > AD ^{d,f}
Semantic fluency score	20.07 ± 5.56	15.80 ± 4.92	12.51 ± 4.84	HC > MCI > AD ^{d,f}
Trail Making Test A, s	36.17 ± 13.31	45.17 ± 22.83	67.33 ± 35.34	AD > MCI > HC ^{d,f}
Trail Making Test B, s	89.17 ± 43.89	131.91 ± 73.02	200.63 ± 87.98	AD > MCI > HC ^{d,f}
Bilateral hippocampal volume, mm ³	5.53 ± 0.69	4.82 ± 0.87	4.12 ± 0.86	HC > MCI > AD ^{d,g}

^aProbability value derived from an analysis of variance test.

^bProbability value derived from a χ^2 test.

^c $p < 0.01$.

^d $p < 0.001$.

^eDonepezil equivalents estimation.

^fProbability value derived from an ANCOVA test controlling for age, sex, and years of education.

^gProbability value derived from an ANCOVA test controlling for age, sex, years of education, and total brain volume.

AD = Alzheimer's disease; ADNI = Alzheimer's Disease Neuroimaging Initiative; ANCOVA = analysis of covariance; F = female; HC = healthy controls; M = male; MCI = mild cognitive impairment; RAVLT = Rey Auditory Verbal Learning Test.

we provide a brief description below. A complete description of these tests and how they were administered is available at the ADNI website (<http://adni.loni.usc.edu/methods/documents>).

- **Rey Auditory Verbal Learning Test (RAVLT):** In this test, a list consisting of 15 words (list A) is read to the participant 5 times. The participant is asked to recall the words after each presentation of list A. Immediately afterward, a 15-word interference list is read to the participant, who is requested to recall the words from this interference list, and then again those from list A. After a 30-minute delay, the participant is inquired to recall the words from list A for the last time and to recognize them from a more extensive list. We considered the

total number of words recalled after each one of the first 5 trials of list A (RAVLT 1–5) as a measure of episodic memory and verbal learning.²⁵ We also considered the total number of words recalled after the 30-minute delay (RAVLT delayed). RAVLT 1–5 constituted the main outcome of our study, as it was considered a more robust measure and showed higher score variability than RAVLT delayed, which was probably affected by a floor effect in AD patients.

- **Mini-Mental State Examination (MMSE):** This is a 30-item questionnaire assessing diverse functions such as orientation, memory, attention, and language. We considered the total score.

TABLE 2. Sociodemographic, Clinical, and Cognitive Data Comparison between HC, MCI, and AD Patients from the ADNI-2 Sample

	ADNI-2, n = 485			Differences
	HC, n = 183	MCI, n = 159	AD, n = 143	
Age, yr	73.44 ± 6.14	72.31 ± 7.55	74.98 ± 8.06	AD > MCI ^{a,b}
Age range	56–89	55–91	56–90	—
Sex, M/F	87/96	85/74	84/59	None ^c
Education, yr	16.49 ± 2.55	16.51 ± 2.60	15.77 ± 2.69	(HC/MCI) > AD ^{a,d}
Ethnicity, white/other	161/22	150/9	131/12	None ^c
Handedness, right-/left-handed	169/14	139/20	131/12	None ^c
Cumulative medication until scan, mg/yr ^e	—	11.01 ± 25.27	40.11 ± 55.40	AD > MCI ^{a,d}
RAVLT sum trials 1–5	45.66 ± 10.30	33.05 ± 10.66	22.02 ± 7.28	HC > MCI > AD ^{d,f}
RAVLT delayed score	7.52 ± 3.99	3.02 ± 3.71	0.69 ± 1.42	HC > MCI > AD ^{d,f}
Mini-Mental State Examination score	28.96 ± 1.29	27.56 ± 1.84	23.08 ± 2.09	HC > MCI > AD ^{d,f}
Immediate Logical Memory score	14.24 ± 2.95	7.07 ± 3.15	4.00 ± 2.72	HC > MCI > AD ^{d,f}
Delayed Logical Memory score	13.41 ± 3.05	4.00 ± 2.71	1.48 ± 1.87	HC > MCI > AD ^{d,f}
Semantic fluency score	21.37 ± 5.33	17.22 ± 4.93	12.15 ± 5.23	HC > MCI > AD ^{d,f}
Trail Making Test A, s	33.32 ± 10.33	41.69 ± 19.27	60.25 ± 32.62	AD > MCI > HC ^{d,f}
Trail Making Test B, s	80.25 ± 38.58	117.14 ± 66.42	190.73 ± 86.81	AD > MCI > HC ^{d,f}
Bilateral hippocampal volume, mm ³	5.75 ± 0.68	4.99 ± 0.93	4.43 ± 0.78	HC > MCI > AD ^{d,g}

^aProbability value derived from an analysis of variance test.

^b $p < 0.01$.

^cProbability value derived from a χ^2 test.

^d $p < 0.001$.

^eDonepezil equivalents estimation.

^fProbability value derived from an ANCOVA test controlling for age, sex, and years of education.

^gProbability value derived from an ANCOVA test controlling for age, sex, years of education, and total brain volume.

AD = Alzheimer's disease; ADNI = Alzheimer's Disease Neuroimaging Initiative; ANCOVA = analysis of covariance; F = female; HC = healthy controls; M = male; MCI = mild cognitive impairment; RAVLT = Rey Auditory Verbal Learning Test.

- Wechsler Logical Memory: In this test, a short story is read once to the participant, who is asked to recall the story immediately and then after 30 to 40 minutes. Scoring is based on the recall of certain phrases and words. We considered immediate and delayed recall scores.
- Semantic fluency: The participant is prompted to name as many animals as possible in 60 seconds. We took the total number of animals named as a measure of semantic fluency.
- Trail Making Test (TMT) A and B: The participant is requested to draw a line connecting circles containing numbers (A) or letters and numbers (B). We obtained the times elapsed to complete each one of the tests and considered these times as measures of processing speed and executive function.

It is important to note that we excluded from the cognitive analyses those participants who had the RAVLT administered >60 days after or before the MRI acquisition, as well as

those not having a valid RAVLT 1–5 score (eg, having a null value in any of the 5 trials). Therefore, we carried out the cognitive analyses in a subsample of 762 participants from ADNI-1 and 453 participants from ADNI-2. In almost all cases, the RAVLT was administered after the MRI acquisition. The median days of difference between MRI and RAVLT was 17 (interquartile range [IQR] = 13) in ADNI-1 and 16 (IQR = 12) in ADNI-2.

Medications

To control the potential confounding effects of those medications prescribed for AD and memory loss, we calculated the cumulative dose intake of these medications for all the participants considering the period ranging from the beginning of the treatment until the date on which the structural image was acquired. Medications used by MCI and AD patients were cholinesterase inhibitors (donepezil, rivastigmine, and galantamine) and an N-methyl-D-aspartate receptor antagonist (memantine). Considering donepezil the drug of reference, we calculated the donepezil dose equivalents for the rest of the medications, in accordance with the following formulas^{26,27}:

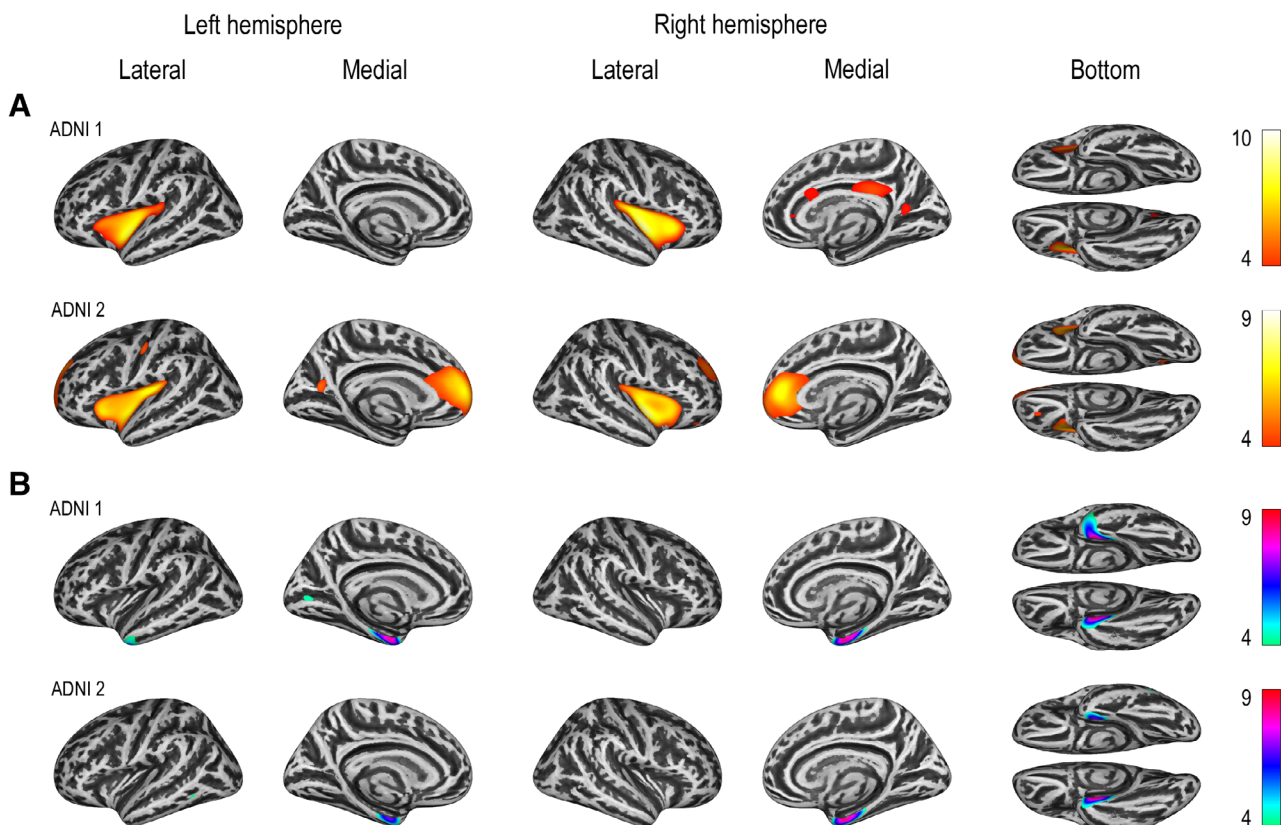


FIGURE 1: Cortical gyrfication differences between healthy controls (HC) and Alzheimer's disease (AD) patients. Lateral, medial, and bottom views of the brain depict the results of the whole-cortex surface-based morphometry analyses of covariance of the gyrfication index maps of the HC and AD groups, controlling for age, sex, and years of education. (A) Increased gyrfication in HC compared with AD. We consistently found increased gyrfication of the bilateral insular cortex in HC in both Alzheimer's Disease Neuroimaging Initiative (ADNI)-1 and ADNI-2 samples. In ADNI-2, we observed increased gyrfication of the bilateral superior frontal cortex as well. (B) Increased gyrfication in AD compared with HC. In this case, we consistently found increased gyrfication of the bilateral entorhinal cortex in AD patients. We employed a vertexwise threshold, familywise error-corrected $p < 0.05$ at the vertex level. The exact regions in which we observed gyrfication differences between HC and AD are listed in the Supplementary Table (a, b). [Color figure can be viewed at www.annalsofneurology.org]

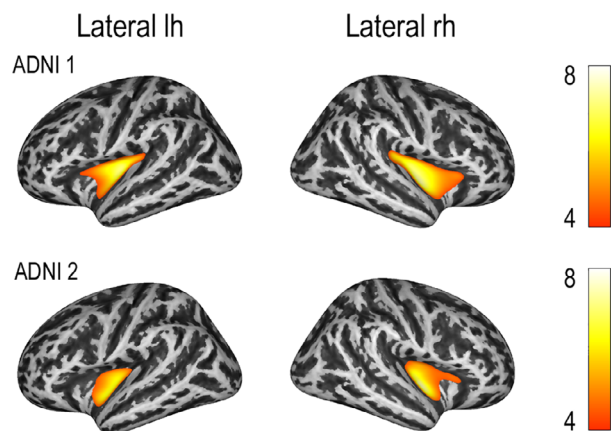


FIGURE 2: Age-related cortical gyrification differences in healthy controls (HC). Lateral views of the brain depict the results of the whole-cortex surface-based morphometry multiple regression analyses of the gyrification index maps of the HC group, using age as a predictor and controlling for sex and years of education. From these analyses, we identified reduced gyrification of the bilateral insular cortex in older HC participants as compared with younger ones. We employed a vertexwise threshold, familywise error–corrected $p < 0.05$ at the vertex level. The exact regions in which we observed age-related gyrification differences are listed in Table 3. ADNI = Alzheimer’s Disease Neuroimaging Initiative; lh = left hemisphere; rh = right hemisphere. [Color figure can be viewed at www.annalsofneurology.org]

- Rivastigmine: dose of rivastigmine / 1.2
- Galantamine: (up to 16mg) dose of galantamine / 3.2; (between 16 and 20mg) dose of galantamine / 2.5; (from 20mg) dose of galantamine / 2.4
- Memantine: equivalent to donepezil

Statistical Analysis

First, we compared sociodemographic, clinical, and cognitive data between HC, MCI, and AD groups, controlling for age, sex, years of education, and total brain volume where appropriate. Second,

we performed whole-cortex SBM analyses of covariance of the GI maps, using diagnostic group (HC, MCI, or AD) as the independent variable and controlling for age, sex, and years of education, to identify localized cortical gyrification differences between groups. Third, aiming to find out whether the gyrification differences observed in the previous analysis were specific to the disease, we analyzed the effects of normal aging on brain gyrification. To this end, we carried out additional whole-cortex SBM multiple regression analyses of the GI maps in the HC group, using age as a predictor and controlling for sex and years of education. Fourth, to explore the relation between cortical gyrification and memory, we performed whole-cortex SBM multiple regression analyses of the GI maps for all the groups, with the RAVLT 1–5 outcome as a predictor, and controlling for age, sex, years of education, and medication (for patients only). Afterward, we conducted linear regression analyses using as a predictor the GI of the whole brain regions in which significant clusters arose from the SBM analyses, controlling for age, sex, years of education, medication, and bilateral hippocampal volume. Fifth, to elucidate whether the gyrification findings in the previous analysis were specific to memory, we performed the same analyses, this time only in the AD group, for the other cognitive outcomes. Lastly, to complement and better understand our gyrification results, some of the previous analyses were repeated employing GM volume and cortical thickness maps. In particular, we analyzed volume and cortical thickness differences between diagnostic groups and the degree to which these parameters were associated with RAVLT 1–5 scores, employing the same methodology as described above. We employed a vertexwise threshold, familywise error (FWE)-corrected $p < 0.05$ at the vertex level, in all the SBM analyses described. In certain cases, duly noted, we employed a more permissive threshold with the purpose of potentially revealing effects showing a trend toward significance. To analyze GM maps, a VBM approach was taken, employing a voxelwise threshold, FWE-corrected $p < 0.05$ at the voxel level, unless noted otherwise. We carried out all the analyses described in this section separately for the ADNI-1 and ADNI-2 samples.

TABLE 3. Exact Locations of the Clusters Showing Age-Related Gyrification Differences in HC from ADNI-1 and ADNI-2

ADNI-1		ADNI-2	
Cluster Size (T)	Region (% of overlap in cluster)	Cluster Size (T)	Region (% of overlap in cluster)
5,663 (7.8)	Right insula (70%)	3,733 (7.6)	Right insula (82%)
	Right superior temporal (13%)		Right superior temporal (12%)
3,908 (7.5)	Left insula (77%)	2,337 (6.5)	Left insula (82%)
	Left superior temporal (11%)		Left superior temporal (16%)

These locations stem from the whole-cortex surface-based morphometry multiple regression analyses of the gyrification index maps of HC, with age as a predictor and controlling for sex and years of education. We employed a vertexwise threshold, familywise error–corrected $p < 0.05$ at the vertex level. Regions with less than 10% overlap with a cluster are not listed. See Figure 2 for a graphical representation of these analyses. ADNI = Alzheimer’s Disease Neuroimaging Initiative; HC = healthy controls.

Results

Sociodemographic, Clinical, and Cognitive Information

Sociodemographic, clinical, and cognitive information for all the participants included in this study is presented in Tables 1 and 2. In the ADNI-1 sample, sex distribution of the MCI group was significantly different than that of the HC and AD groups. In the ADNI-2 sample, AD

patients were significantly older than MCI. In both ADNI-1 and ADNI-2, AD patients were less educated than the rest. As expected, the performance on all cognitive tests was gradually impaired in MCI and AD patients in both samples. A head-to-head comparison of the 2 samples showed that HC participants from ADNI-1 were significantly older ($p < 0.001$) and had better MMSE scores ($p = 0.018$) than those from ADNI-2. MCI participants

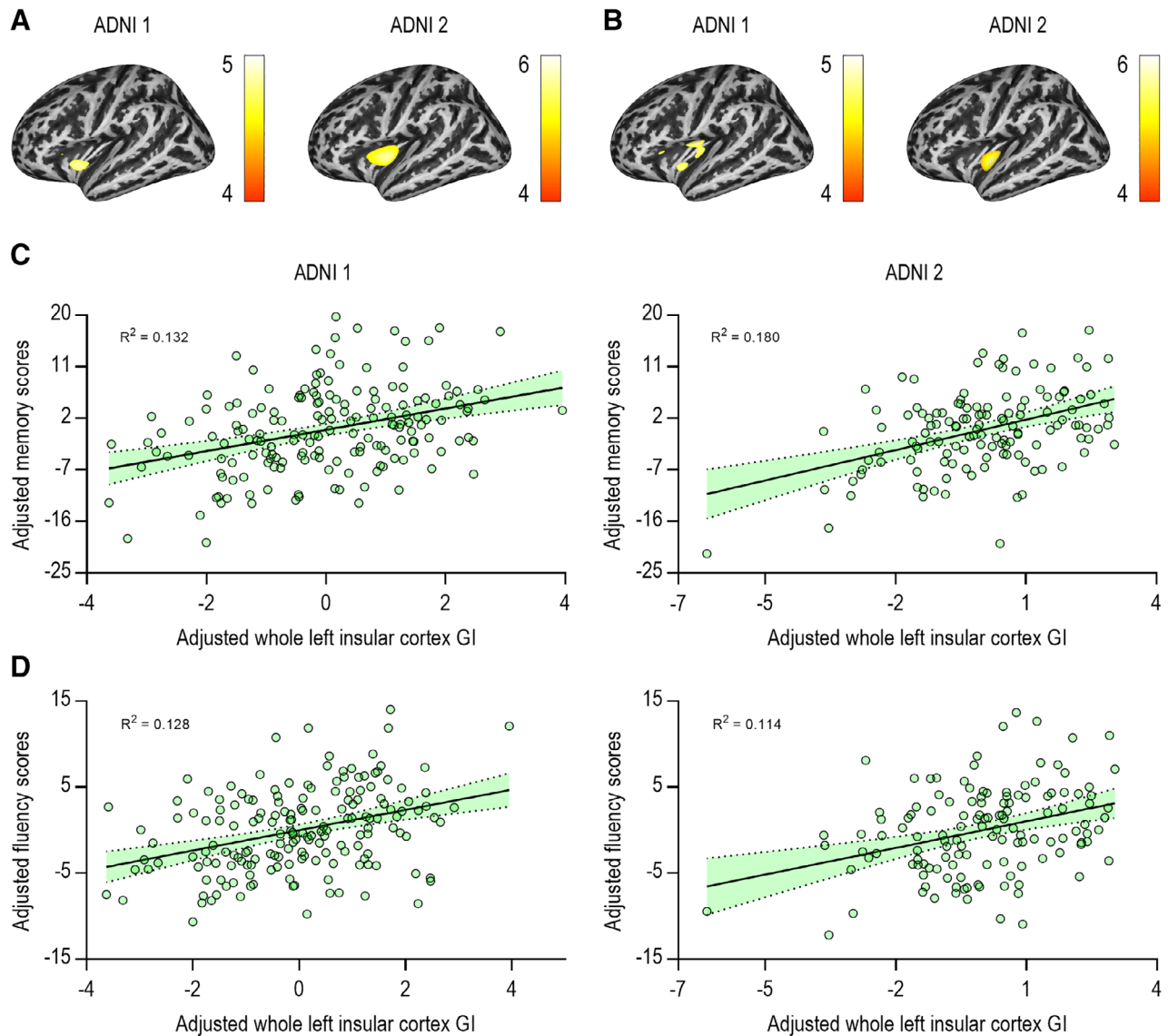


FIGURE 3: Higher gyrfication of the left insular cortex is associated with better memory function and semantic fluency in Alzheimer's disease (AD) patients. (A, B) Lateral views of the left hemisphere of the brain depicting the results of the whole-cortex surface-based morphometry (SBM) multiple regression analyses for cognition in AD participants, controlling for age, sex, years of education, and medication. We found clusters of increased gyrfication located at the left insular cortex associated with better episodic memory and verbal learning (A) and semantic fluency (B), which is highly reliant on episodic memory, in AD patients. We employed a vertexwise threshold, familywise error-corrected $p < 0.05$ at the vertex level. **(C, D)** Scatter plots representing the linear regression analyses between gyrfication index (GI) of the whole left insular cortex and episodic memory and semantic fluency scores. Consistent with the SBM analyses, we found that increased gyrfication of the whole left insular cortex was also associated with better episodic memory and verbal learning scores (C) and semantic fluency (D) in AD patients, controlling for the aforementioned potential confounding factors. See Figure 5 for related analyses. ADNI = Alzheimer's Disease Neuroimaging Initiative. [Color figure can be viewed at www.annalsofneurology.org]

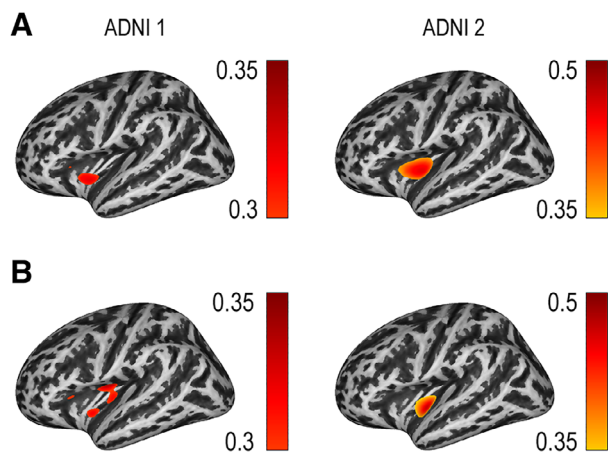


FIGURE 4: Correlation coefficient maps depicting the effect sizes of the whole-cortex surface-based morphometry multiple regression analyses for cognition in Alzheimer's disease patients in both Alzheimer's Disease Neuroimaging Initiative (ADNI)-1 and ADNI-2 samples (see Fig 3). (A) Effect sizes of the episodic memory and verbal learning tests. (B) Effect sizes of the semantic fluency tests. [Color figure can be viewed at www.annalsofneurology.org]

from ADNI-1 were significantly older ($p < 0.001$), less educated ($p = 0.001$), and had worse MMSE scores ($p = 0.016$) than those from ADNI-2, and the sex distribution was different ($p = 0.029$). Finally, AD participants from ADNI-1 were less educated ($p < 0.001$) and less medicated ($p = 0.014$) than those from ADNI-2, but there were no significant differences between samples in any of the cognitive tests.

Cortical Gyrfication Differences between Groups

We found a consistent gyrfication decrease mainly located at the bilateral insular cortex of AD patients as compared with

HC, in both ADNI-1 and ADNI-2 samples (Fig 1A and Supplementary Table, a). The bilateral superior frontal cortex also appeared hypogyrficated in the AD patients of the ADNI-2 sample, although we did not observe this in ADNI-1. In contrast, we found a consistent gyrfication increase mainly at the bilateral entorhinal cortex of the AD patients of ADNI-1 and ADNI-2 (see Fig 1B and Supplementary Table, b). Overall, MCI patients showed an intermediate cortical gyrfication pattern between HC and AD patients (see Supplementary Table, c–f).

Changes in Cortical Gyrfication with Normal Aging

We observed a prominent decrease in the gyrfication of the bilateral insular cortex associated with increasing age in the HC group of both ADNI samples (Fig 2 and Table 3). Conversely, only 2 very small clusters, which included the left supramarginal and the right inferior temporal and fusiform cortices, showed increased gyrfication in the older participants of the ADNI-2 sample, and no regions of increased gyrfication with increasing age arose in the ADNI-1 sample.

Association between Cortical Gyrfication and Episodic Memory and Verbal Learning

Whereas we did not find significant associations between cortical gyrfication and RAVLT 1–5 scores in the HC and MCI groups, we found a cluster of increased gyrfication located at the left insular cortex that was significantly associated with better RAVLT 1–5 scores in AD patients, in both the ADNI-1 and ADNI-2 samples (Fig 3A; the estimated effect sizes are depicted in Fig 4A). We also found, through linear regression analyses, that the GI of the whole left insular cortex consistently correlated with RAVLT 1–5

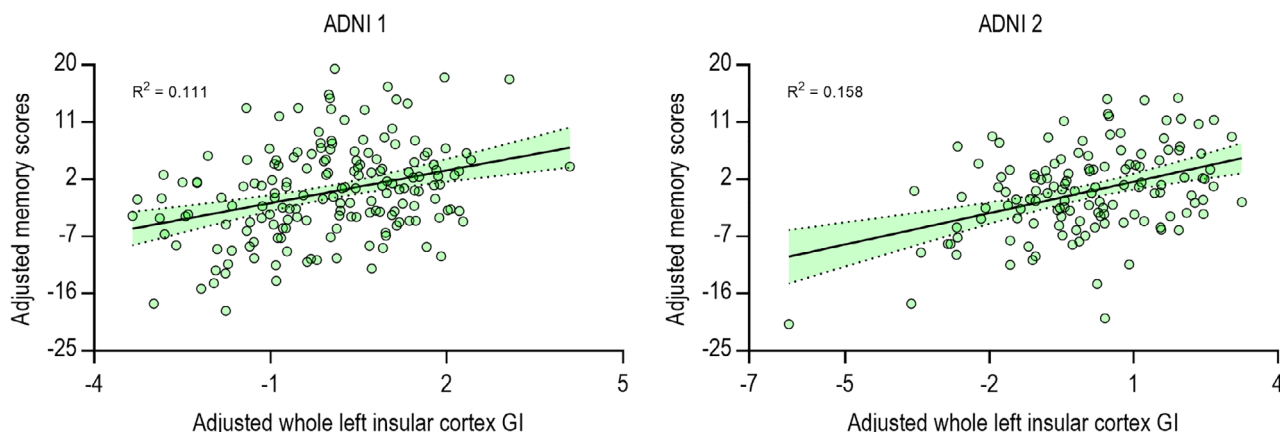


FIGURE 5: Scatter plots depicting the linear regression analyses between the gyrfication index (GI) of the whole left insular cortex and episodic memory scores in Alzheimer's disease patients. Increased gyrfication of the whole left insular cortex was still associated with better episodic memory and verbal learning scores in both Alzheimer's Disease Neuroimaging Initiative (ADNI)-1 and ADNI-2 samples after we included bilateral hippocampal volume as an additional predictor, controlling for age, sex, years of education, and medication. [Color figure can be viewed at www.annalsofneurology.org]

scores (ADNI-1: $\beta = 0.380$, $p < 0.001$; ADNI-2: $\beta = 0.445$, $p < 0.001$; see Fig 3B), even after including bilateral hippocampal volume as an additional predictor (ADNI-1: $\beta = 0.352$, $p < 0.001$; ADNI-2: $\beta = 0.415$, $p < 0.001$; Fig 5). Indeed, gyrfication of the whole left insular cortex was a better predictor of RAVLT 1–5 scores than hippocampal volumes. Interestingly, we observed a cluster of increased gyrfication at the left insular cortex associated with better RAVLT 1–5 scores in MCI patients of ADNI-1 and ADNI-2, but not in HC, after repeating the SBM multiple regression analyses with a lower significance threshold (uncorrected cluster-level threshold defined by $p < 0.001$). Gyrfication of the whole left insular cortex also correlated with RAVLT 1–5 scores in MCI patients, although this association was much weaker than that observed in AD patients (ADNI-1: $\beta = 0.150$, $p = 0.005$;

ADNI-2: $\beta = 0.281$, $p = 0.001$). Overall, these results with the MCI group suggest a trend-level association between increased gyrfication of the left insular cortex and better episodic memory in these patients.

Association between Cortical Gyrfication and Other Cognitive Outcomes

Aiming to determine whether the association between left insular cortex folding and cognition was specific to RAVLT 1–5 scores, we carried out additional SBM analyses for several other cognitive outcomes, only in the AD group. We found cortical gyrfication associations only for the animal fluency test, in which clusters of increased gyrfication, mainly located at the left insular cortex, were positively correlated with semantic fluency scores in both ADNI-1 and ADNI-2 (see Fig 3C, D; the estimated effect

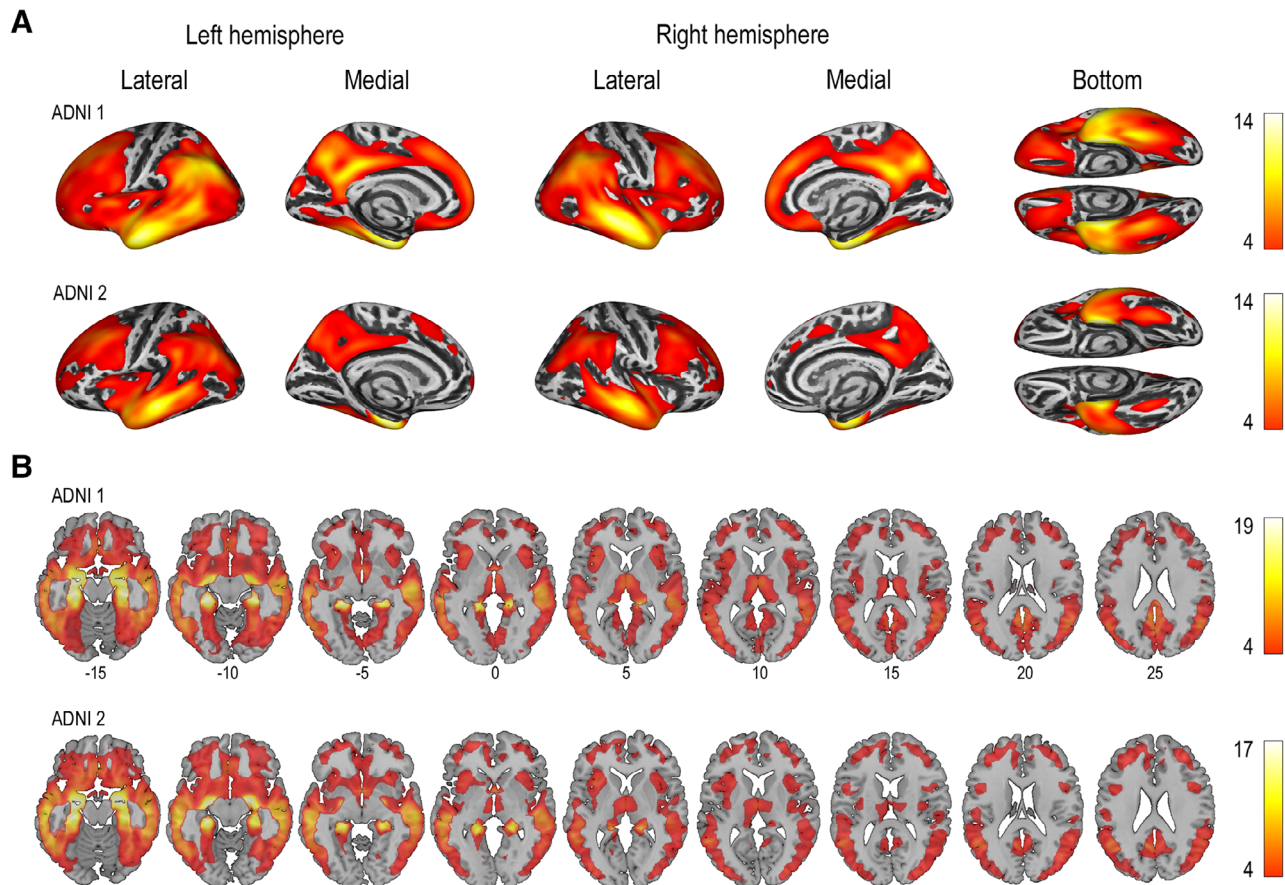


FIGURE 6: Cortical thickness and gray matter (GM) volume differences between healthy controls (HC) and Alzheimer's disease (AD) patients. (A) Lateral, medial, and bottom views of the brain depicting the results of the whole-cortex surface-based morphometry analyses of covariance (ANCOVAs) of the cortical thickness maps of the HC and AD groups. We employed a vertexwise threshold, familywise error (FWE)-corrected $p < 0.05$ at the vertex level. (B) Axial views of the brain depicting the results of the whole-brain voxel-based morphometry ANCOVAs of the GM volume maps of the HC and AD groups. We employed a voxelwise threshold, FWE-corrected $p < 0.05$ at the voxel level. The numbers below the first row of axial images indicate the z Montreal Neurological Institute coordinate. In both the Alzheimer's Disease Neuroimaging Initiative (ADNI)-1 and ADNI-2 samples, we observed a generalized cortical thinning and GM atrophy in AD patients compared with HC, which was more prominent in the medial temporal lobe region. All these analyses were controlled for age, sex, and years of education. [Color figure can be viewed at www.annalsofneurology.org]

sizes are depicted in Fig 4B). In ADNI-1, we observed an additional cluster that included the right postcentral and insular cortices. Otherwise, no cortical regions were associated with any of the other outcome measures at the stipulated significance threshold, save for a very small cluster of increased gyrification located at the right lingual cortex, which was associated with impaired immediate Logical Memory. When we employed lower significance thresholds in the SBM analyses, we found regions of increased gyrification at the left insular cortex to be associated with better scores on RAVLT delayed, immediate and delayed Logical Memory, and TMT-B, suggesting that trend-level associations may exist, although we found most of these associations only in the ADNI-2 sample. MMSE and TMT-A tests did not show any association with left insular cortex gyrification at all.

Value of Gyrification as a Cerebral Parameter in AD versus Other Measures

To assess the utility of gyrification as a cerebral parameter in AD, we repeated the main analyses employing more conventional measures, namely GM volume and cortical thickness. A widespread decrease in GM volume and cortical thickness was observed in the brains of AD patients as compared with HC, with the medial temporal lobe showing the most prominent differences (Fig 6). This is in opposition to the differences between patients and controls reported in gyrification analyses, which were more localized and mainly restricted to the insular and entorhinal cortices employing the same level of significance and even a more permissive threshold (uncorrected cluster-level threshold defined by $p < 0.001$, data not shown). The spatial pattern of global atrophy and cortical thinning was similar in ADNI-1 and ADNI-2, and no regions of increased volume or cortical thickness were observed in AD patients. Expectedly, reduced volumes of the temporal lobe (including its medial part), especially from the left hemisphere, were associated with poorer performance in the RAVLT 1–5 task in AD patients. This was more evident in more permissive VBM analyses (corrected cluster-level threshold defined by $p < 0.001$). Cortical thinning of several cortical regions, namely superior and middle temporal, inferior parietal, supramarginal, and precuneus, was also associated with lower RAVLT 1–5 scores. Conversely, no associations between volume or cortical thickness and RAVLT 1–5 scores were found in HC.

Discussion

In the present report, we showed that the main cortical gyrification differences between HC and AD patients were located at the insular and the entorhinal cortices, which were revealed to be hypo- and hypergyrified,

respectively, in patients. Moreover, we found that the degree of gyrification of the insular cortex was associated with better episodic memory and verbal learning abilities only in AD patients. Overall, MCI patients showed an intermediate pattern between HC and AD patients. We consistently observed all these findings in 2 large, independent samples.

This is the first study to show a consistent gyrification increase of the bilateral entorhinal cortex and adjacent regions, such as the parahippocampal cortex, of MCI and AD patients. Although Lebed et al¹⁴ reported similar results, their findings were highly inconsistent (ie, increases/decreases in the gyrification degree of these regions were not stable between groups), probably because of the small sample employed. In contrast, our finding of MCI and AD patients presenting less gyrification in the insular cortex and, to a lesser extent, adjacent regions such as the superior temporal cortex, is clearly in agreement with previous studies showing a widening of the Sylvian fissure,^{12,15} in which the insular cortex is located, and the superior temporal sulcus^{12,15,16} of MCI and/or AD patients. Other studies^{17,18} reported similar results employing alternative means to measure gyrification. Notably, Cai et al²⁸ proposed the width of the Sylvian fissure as a useful biomarker for detecting AD in its earlier stages. Some studies also reported a widening of the superior frontal sulcus of patients,^{12,15} which is in line with our finding of decreased gyrification in this cortical region; however, this result was inconsistent, as we observed it in only 1 of the 2 samples analyzed, and it would therefore require further research. It is interesting to note that differences in the gyrification of the entorhinal cortex were not significant between the MCI and AD groups, suggesting that most of the hypergyrification process in this region must occur during the early stages of the disease. In contrast, insular cortex differences were prominent in all the group comparisons, whereas decreased gyrification of the superior frontal cortex was observed only in AD patients when compared to HC, but not in MCI. Overall, cortical gyrification changes in dementia seem to be congruent with the brain atrophy pattern observed in these patients, in which the disease affects the medial temporal lobe in its early stages and then spreads to more frontal regions.²⁹

Reduced gyrification of the bilateral insular cortex was also observed in older HC participants compared with younger ones. This is consistent with Hogstrom et al,⁴ who found a widespread cortical gyrification decrease as a function of age in a large sample of healthy participants with ages ranging from 20 to 85 years. They theorized that this was likely a consequence of progressive widening of the cortical sulci. Our result, in a sample of HC encompassing a narrower age interval (56–90 years), may indicate that gyrification decreases in the elderly are

particularly relevant in the insular cortex. Therefore, hypogyrfication of the insular cortex, which is possibly caused by a widening of the Sylvian fissure, as mentioned above, does not seem to be specific to AD. Rather, the presumably normal process of widening of the Sylvian fissure seems to be accelerated in AD. In contrast, hypergyrfication of the entorhinal cortex appears to be quite specific to dementia, as it was observed in MCI and AD patients, but not in older HC.

The observed increased gyrfication of the bilateral entorhinal cortex and adjacent regions initially appears counterintuitive. The most straightforward explanation for this finding is that the geometry of the cortex changes as a consequence of the atrophy in this region, which is more prominent than in other areas in AD patients, as seen in the volumetric and cortical thickness analyses. However, it is remarkable that this is the only region to show increased gyrfication even though the atrophy is global and some areas, such as the insular and superior temporal cortices, show a certain degree of cortical thinning, yet are rather hypogyrficated. Hence, we may speculate that 2 different mechanisms, not mutually exclusive, could partly account for the distinct hypergyrfication of the entorhinal cortex. The first one would involve the creation of new neurons, that is, neurogenesis, in an attempt to regenerate the lost brain tissue. This process would force the brain to make room for the newly created neurons in an otherwise atrophied, and therefore smaller, cerebral region, which could be attained by increasing the folding at this location. It is important to note that the dentate gyrus of the hippocampus, which is located very close to the entorhinal cortex and strongly connected with it through the perforant pathway,³⁰ is one of the very few cerebral regions, if not the only one, in which adult neurogenesis has been observed.³¹ It has been shown that lesions in the entorhinal cortex may induce hippocampal neurogenesis,³² thus emphasizing the importance of the connectivity between these two regions. Interestingly, hypergyrfication of the dentate gyrus has been shown to be associated with neurogenesis in this region in a rat model of epilepsy.³³ Further supporting our view, an overexpression of marker proteins of neurogenesis has been found postmortem in the hippocampus of AD patients, and this expression seemed to positively correlate with disease severity,³⁴ suggesting that the creation of new neurons in these patients outpaces that observed in healthy conditions. However, this is a subject of current debate, as a recent article reported decreased neurogenesis in AD.³⁵ In light of this controversy, we may wonder whether even a small number of new neurons enclosed in a highly and increasingly atrophied brain area are enough to modify its folding properties.

The second suggested mechanism involves the rewiring process that the brain may initiate in an attempt

to restore the connections that are hypothetically lost as a consequence of brain atrophy. In this regard, there appears to be a strong association between connectivity and gyrfication,³⁶ and maximizing the folding of a particular area would presumably favor the formation of new connections.³⁷ It is appropriate to remember that the entorhinal cortex and adjacent regions are affected from a very early stage of the disease; hence, at the time at which MRI was performed in the patients analyzed here, these two hypothetical mechanisms would have been operating long enough to detect their effects, that is, in this case, cortical gyrfication changes. It is important to keep in mind, however, that from the evidence obtained in this structural neuroimaging study, it is impossible to determine whether these mechanisms are actually taking place. Therefore, the proposed mechanisms are purely speculative and have to be seen exclusively as alternative explanations. These could be tested with the appropriate experimental setting, such as, for example, a postmortem sample of AD in which both the expression of marker proteins of neurogenesis and the degree of gyrfication of the entorhinal cortex were analyzed. Finally, because the insular and entorhinal cortices are strongly interconnected,^{38–40} we cannot disregard the potential existence of interactive mechanisms between these two regions that could explain at once their opposite gyrfication trends in AD. This is undoubtedly an interesting question for further research.

The importance of considering the folding characteristics of the insular cortex in AD is further emphasized by our results in cognition. As far as we know, this is the first report in which the degree of gyrfication of a cortical region is associated with the mnemonic performance of AD patients. Specifically, AD patients presenting a higher degree of gyrfication of the left insular cortex consistently showed better episodic memory and verbal learning abilities than those patients with a less gyrficated left insula. Increased gyrfication in this region was also associated with better scores in a task of verbal semantic fluency, which is also highly dependent on episodic memory.⁴¹ It is worth noting that, overall, the effect sizes of these associations may be regarded as moderate. This suggests that although the degree of gyrfication of the left insular cortex does not fully account for the variation of the memory and verbal fluency scores, which is probably explained to a greater extent by widespread cerebral atrophy, it is nevertheless a highly specific and important cognitive biomarker in AD. Notably, gyrfication of the left insular cortex was a better indicator of memory and learning performance than the bilateral hippocampal volume, which is a key structure for episodic memory.^{25,42} Consistent with the implication of episodic memory on semantic fluency, these tasks are also highly reliant on the temporal lobe,

particularly the medial temporal lobe.^{41,43} It is remarkable that the association between left insular cortex gyrification and memory performance was not seen in HC, and that, in MCI patients, this association appeared to exist although much less robustly than that observed in AD patients. This suggests that the insular cortex may progressively assume memory functions as the disease spreads, probably because the increasingly atrophied medial temporal lobe cannot sustain them. Congruently, some functional MRI studies have evidenced the presence of compensatory mechanisms, consisting of increased functional brain activation during an episodic memory task, in healthy participants with reduced memory performance,⁴⁴ healthy participants at high risk of AD,^{45,46} and patients with AD.^{47,48} These increases in brain activation occur predominantly in the frontal lobe, but have also been observed in the left insular cortex.⁴⁴ An overactivation of the left insular and left inferior frontal cortices was also found to protect memory function in healthy participants at high risk of AD during resting state.⁴⁹ Additionally, the strength of the connections between the insula and several frontal regions has been associated with better episodic memory in amnesic MCI patients.⁵⁰ In light of our results and previous literature, the insular cortex appears to be fundamentally and specifically involved in the memory function of demented patients, either by participating directly in the memory process or by facilitating the engagement of frontal regions. Therefore, it may be hypothesized that greater folding of the left insular cortex in AD patients indicates that functional compensatory mechanisms are working properly. Although the implication of the left insular cortex in other cognitive functions cannot be fully ruled out, associations between gyrification in this region and other cognitive tests were observed to a smaller extent and were highly inconsistent. Future studies should address this subject in a more comprehensive way, using a larger battery of neuropsychological tests spanning more cognitive functions.

It is worth emphasizing the importance of quantifying and analyzing cortical gyrification in AD. The analysis of this parameter led to unique and more concise findings than the analysis of more typical parameters, namely brain volume and cortical thickness, which seem to roughly reflect the global atrophy of the diseased brain. As a result, we were able to reveal regions that are likely to be important in AD and that would have gone unnoticed with those more conventional brain measures. This is the case of the insular cortex, which did not show up as a relevant finding in the brain volume or cortical thickness analyses, but that was practically the only region showing a decreased degree of folding in AD and an important association with mnemonic performance in these patients.

While the findings presented here contribute to further understanding of the biological aspects of neurodegeneration and AD in particular, they can also be of interest for clinical practice. The quantification of the degree of folding of the insular and entorhinal cortices may be employed as a useful neuroanatomical marker that could be helpful as an adjuvant diagnostic tool and as a means to monitor the progression of the disease. Moreover, identifying the precise mechanisms that are behind the cortical folding changes in these areas, about some of which we have hypothesized, may be of great importance for the development of new therapies to slow down the disease or to alleviate its symptoms.

The present study has several strengths. First, we processed and analyzed 2 large, independent participant samples, thereby enhancing the reliability and generalizability of the results reported. Second, we employed a whole-cortex methodology, which allowed us to evaluate cortical gyrification from a wider and unbiased perspective. Third, we carried out all the analyses controlling for important potentially confounding variables, namely age, sex, years of education, and medication, in an attempt to ensure as much as possible that the observed effects were truly explained by our variables of interest. On the other hand, the main limitation of this study is its cross-sectional nature, meaning that intrasubject changes in cortical gyrification could not be assessed. An additional limitation is that brain structural images were acquired in several different scanners, which is an uncontrolled confounding factor, although the large sample employed would be expected to have attenuated its potential effects. Future studies may analyze longitudinal gyrification changes in patients with AD, and how they differ from HC participants. Moreover, as noted throughout this section, future investigations may examine in depth the relations between the gyrification of the entorhinal cortex and both neurogenesis and neuronal connectivity, as well as between neurocognitive performance and insular cortex folding.

In conclusion, we have shown, for the first time, hypergyrification of the entorhinal cortex as a distinctive feature of AD brains. AD patients also present a hypogyrification of the insular cortex, which is consistently associated with memory impairment. Overall, this article emphasizes the important role of the insular and entorhinal cortices in AD. Cortical folding changes in these areas could be a consequence of important biological mechanisms taking place in the brain during neurodegeneration.

Acknowledgment

Data collection and sharing for this project was funded by the ADNI (NIH National Institute on Aging grant U01

AG024904) and Department of Defense (DOD) ADNI (Department of Defense award number W81XWH-12-2-0012). ADNI is funded by the NIH National Institute on Aging, the NIH National Institute of Biomedical Imaging and Bioengineering, and generous contributions from the following: AbbVie, Alzheimer's Association, Alzheimer's Drug Discovery Foundation, Araclon Biotech, BioClinica, Biogen, Bristol-Myers Squibb Company, CereSpir, Cogstate, Eisai, Elan Pharmaceuticals, Eli Lilly and Company, EuroImmun, F. Hoffmann-La Roche and its affiliated company Genentech, Fujirebio, GE Healthcare, IXICO, Janssen Alzheimer Immunotherapy Research & Development, Johnson & Johnson Pharmaceutical Research & Development, Lumosity, Lundbeck, Merck & Co, Meso Scale Diagnostics, NeuroRx Research, Neurotrack Technologies, Novartis Pharmaceuticals Corporation, Pfizer, Piramal Imaging, Servier, Takeda Pharmaceutical Company, and Transition Therapeutics. The Canadian Institutes of Health Research is providing funds to support ADNI clinical sites in Canada. Private sector contributions are facilitated by the Foundation for the National Institutes of Health (www.fnih.org). The grantee organization is the Northern California Institute for Research and Education, and the study is coordinated by the Alzheimer's Therapeutic Research Institute at the University of Southern California. ADNI data are disseminated by the Laboratory for Neuro Imaging at the University of Southern California. IDIBAPS is supported by the CERCA program (Generalitat de Catalunya).

Author Contributions

C.N. and C.S.-O. contributed to the conception and design of the study. C.N. analyzed the data. All authors contributed to drafting the manuscript and figures.

Potential Conflicts of Interest

Nothing to report.

References

1. Yang J, Pan P, Song W, et al. Voxewise meta-analysis of gray matter anomalies in Alzheimer's disease and mild cognitive impairment using anatomic likelihood estimation. *J Neurol Sci* 2012;316:21–29.
2. Fischl B, Rajendran N, Busa E, et al. Cortical folding patterns and predicting cytoarchitecture. *Cereb Cortex* 2008;18:1973–1980.
3. Ronan L, Fletcher PC. From genes to folds: a review of cortical gyrfication theory. *Brain Struct Funct* 2015;220:2475–2483.
4. Hogstrom LJ, Westlye LT, Walhovd KB, Fjell AM. The structure of the cerebral cortex across adult life: age-related patterns of surface area, thickness, and gyrfication. *Cereb Cortex* 2013;23:2521–2530.
5. Luders E, Narr KL, Bilder RM, et al. Mapping the relationship between cortical convolution and intelligence: effects of gender. *Cereb Cortex* 2008;18:2019–2026.
6. Gregory MD, Kippenhan JS, Dickinson D, et al. Regional variations in brain gyrfication are associated with general cognitive ability in humans. *Curr Biol* 2016;26:1301–1305.
7. Tadayon E, Pascual-Leone A, Santarnecchi E. Differential contribution of cortical thickness, surface area, and gyrfication to fluid and crystallized intelligence. *Cereb Cortex* 2020;30:215–225.
8. Zilles K, Palomero-Gallagher N, Amunts K. Development of cortical folding during evolution and ontogeny. *Trends Neurosci* 2013;36:275–284.
9. Striedter GF, Srinivasan S, Monuki ES. Cortical folding: when, where, how, and why? *Annu Rev Neurosci* 2015;38:291–307.
10. Im K, Lee JM, Seo SW, et al. Sulcal morphology changes and their relationship with cortical thickness and gyral white matter volume in mild cognitive impairment and Alzheimer's disease. *Neuroimage* 2008;43:103–113.
11. Cash DM, Melbourne A, Modat M, et al. Cortical folding analysis on patients with Alzheimer's disease and mild cognitive impairment. *Med Image Comput Comput Assist Interv* 2012;15:289–296.
12. Liu T, Lipnicki DM, Zhu W, et al. Cortical gyrfication and sulcal spans in early stage Alzheimer's disease. *PLoS One* 2012;7:e31083.
13. Reiner P, Jouvent E, Duchesnay E, et al. Sulcal span in Alzheimer's disease, amnesic mild cognitive impairment, and healthy controls. *J Alzheimers Dis* 2012;29:605–613.
14. Lebed E, Jacova C, Wang L, Beg MF. Novel surface-smoothing based local gyrfication index. *IEEE Trans Med Imaging* 2013;32:660–669.
15. Liu T, Sachdev PS, Lipnicki DM, et al. Longitudinal changes in sulcal morphology associated with late-life aging and MCI. *Neuroimage* 2013;74:337–342.
16. Hamelin L, Bertoux M, Bottlaender M, et al. Sulcal morphology as a new imaging marker for the diagnosis of early onset Alzheimer's disease. *Neurobiol Aging* 2015;36:2932–2939.
17. Wang T, Shi F, Jin Y, et al. Abnormal changes of brain cortical anatomy and the association with plasma MicroRNA107 level in amnesic mild cognitive impairment. *Front Aging Neurosci* 2016;8:112.
18. Ruiz de Miras J, Costumero V, Belloch V, et al. Complexity analysis of cortical surface detects changes in future Alzheimer's disease converters. *Hum Brain Mapp* 2017;38:5905–5918.
19. Dahnke R, Yotter RA, Gaser C. Cortical thickness and central surface estimation. *Neuroimage* 2013;65:336–348.
20. Luders E, Thompson PM, Narr KL, et al. A curvature-based approach to estimate local gyrfication on the cortical surface. *Neuroimage* 2006;29:1224–1230.
21. Desikan RS, Ségonne F, Fischl B, et al. An automated labeling system for subdividing the human cerebral cortex on MRI scans into gyral based regions of interest. *Neuroimage* 2006;31:968–980.
22. Seiger R, Ganger S, Kranz GS, et al. Cortical thickness estimations of FreeSurfer and the CAT12 toolbox in patients with Alzheimer's disease and healthy controls. *J Neuroimaging* 2018;28:515–523.
23. Besteher B, Gaser C, Spalthoff R, Nenadić I. Associations between urban upbringing and cortical thickness and gyrfication. *J Psychiatr Res* 2017;95:114–120.
24. Spalthoff R, Gaser C, Nenadić I. Altered gyrfication in schizophrenia and its relation to other morphometric markers. *Schizophr Res* 2018;202:195–202.
25. Saury JM, Emanuelson I. Neuropsychological assessment of hippocampal integrity. *Appl Neuropsychol Adult* 2017;24:140–151.
26. Grossberg GT. Cholinesterase inhibitors for the treatment of Alzheimer's disease: getting on and staying on. *Curr Ther Res Clin Exp* 2003;64:216–235.
27. Sasaki S, Horie Y. The effects of an uninterrupted switch from donepezil to galantamine without dose titration on behavioral and

- psychological symptoms of dementia in Alzheimer's disease. *Dement Geriatr Cogn Dis Extra* 2014;4:131–139.
28. Cai K, Xu H, Guan H, et al. Identification of early-stage Alzheimer's disease using sulcal morphology and other common neuroimaging indices. *PLoS One* 2017;12:e0170875.
 29. Scahill RI, Schott JM, Stevens JM, et al. Mapping the evolution of regional atrophy in Alzheimer's disease: unbiased analysis of fluid-registered serial MRI. *Proc Natl Acad Sci U S A* 2002;99:4703–4707.
 30. Witter MP. The perforant path: projections from the entorhinal cortex to the dentate gyrus. *Prog Brain Res* 2007;163:43–61.
 31. Spalding KL, Bergmann O, Alkass K, et al. Dynamics of hippocampal neurogenesis in adult humans. *Cell* 2013;153:1219–1227.
 32. Gama Sosa MA, Wen PH, De Gasperi R, et al. Entorhinal cortex lesioning promotes neurogenesis in the hippocampus of adult mice. *Neuroscience* 2004;127:881–891.
 33. Magagna-Poveda A, Moretto JN, Scharfman HE. Increased gyrification and aberrant adult neurogenesis of the dentate gyrus in adult rats. *Brain Struct Funct* 2017;222:4219–4237.
 34. Jin K, Peel AL, Mao XO, et al. Increased hippocampal neurogenesis in Alzheimer's disease. *Proc Natl Acad Sci U S A* 2004;101:343–347.
 35. Moreno-Jiménez EP, Flor-García M, Terreros-Roncal J, et al. Adult hippocampal neurogenesis is abundant in neurologically healthy subjects and drops sharply in patients with Alzheimer's disease. *Nat Med* 2019;25:554–560.
 36. Van Essen DC. A tension-based theory of morphogenesis and compact wiring in the central nervous system. *Nature* 1997;385:313–318.
 37. Ruppin E, Schwartz EL, Yeshurun Y. Examining the volume efficiency of the cortical architecture in a multi-processor network model. *Biol Cybern* 1993;70:89–94.
 38. Bonthius DJ, Solodkin A, Van Hoesen GW. Pathology of the insular cortex in Alzheimer's disease depends on cortical architecture. *J Neuropathol Exp Neurol* 2005;64:910–922.
 39. Ghaziri J, Tucholka A, Girard G, et al. The corticocortical structural connectivity of the human insula. *Cereb Cortex* 2017;27:1216–1228.
 40. Witter MP, Doan TP, Jacobsen B, et al. Architecture of the entorhinal cortex: a review of entorhinal anatomy in rodents with some comparative notes. *Front Syst Neurosci* 2017;11:46.
 41. Greenberg DL, Keane MM, Ryan L, Verfaellie M. Impaired category fluency in medial temporal lobe amnesia: the role of episodic memory. *J Neurosci* 2009;29:10900–10908.
 42. Moradi E, Hallikainen I, Hänninen T, et al. Rey's auditory verbal learning test scores can be predicted from whole brain MRI in Alzheimer's disease. *Neuroimage Clin* 2016;13:415–427.
 43. Baldo JV, Schwartz S, Wilkins D, Dronkers NF. Role of frontal versus temporal cortex in verbal fluency as revealed by voxel-based lesion symptom mapping. *J Int Neuropsychol Soc* 2006;12:896–900.
 44. Daselaar SM, Veltman DJ, Rombouts SA, et al. Neuroanatomical correlates of episodic encoding and retrieval in young and elderly subjects. *Brain* 2003;126:43–56.
 45. Bookheimer SY, Strojwas MH, Cohen MS, et al. Patterns of brain activation in people at risk for Alzheimer's disease. *N Engl J Med* 2000;343:450–456.
 46. Bondi MW, Houston WS, Eyler LT, Brown GG. fMRI evidence of compensatory mechanisms in older adults at genetic risk for Alzheimer's disease. *Neurology* 2005;64:501–508.
 47. Grady CL, McIntosh AR, Beig S, et al. Evidence from functional neuroimaging of a compensatory prefrontal network in Alzheimer's disease. *J Neurosci* 2003;23:986–993.
 48. Rémy F, Mirrashed F, Campbell B, Richter W. Verbal episodic memory impairment in Alzheimer's disease: a combined structural and functional MRI study. *Neuroimage* 2005;25:253–266.
 49. Lin F, Ren P, Lo RY, et al. Insula and inferior frontal gyrus' activities protect memory performance against Alzheimer's disease pathology in old age. *J Alzheimers Dis* 2017;55:669–678.
 50. Xie C, Bai F, Yu H, et al. Abnormal insula functional network is associated with episodic memory decline in amnesic mild cognitive impairment. *Neuroimage* 2012;63:320–327.